THE WAVELET APPROACH IN RADAR IMAGING AND ITS PHYSICAL INTERPRETATION

Jacqueline BERTRAND[1], Pierre BERTRAND[2], Jean-Philippe OVARLEZ[2]

[1] **CNRS and University Paris VII, LPTM, 75251 PARIS, France**

[2] **ONERA DES, BP 72, 92322 CHATILLON, France**

Abstract: Radar Imaging is developed using a colored and non isotropic bright points model. The study of the response of this model to simple transformations (space shift, scale change, rotation) allows to define a wavelet analysis which depends on the physical dimension of the problem. This analysis gives the position of bright points versus the frequency and the angle at and under which they reflect. It has been implemented using an original tool, the Mellin transform

1. GENERAL PRINCIPLES OF RADAR IMAGING

The radar imaging techniques are powerful analysis tools which allow to characterize the backscattering properties of illuminated targets in order, if necessary, to mask or, on the contrary, to amplify the echo of some parts of the targets. Illuminating a target by a plane wave using a coherent radar in anechoic chamber, the values of the complex backscattering coefficients $H(\vec{k})$ are collected for each frequency and each angles of presentation of the target. The square modulus of $H(\vec{k})$ obtained for the wave vector $\vec{k}$ in the target coordinates system:

$$\vec{k} = \frac{2f}{c} \begin{vmatrix} \cos\theta \cos\Psi \\ \sin\theta \cos\Psi \\ \sin\Psi \end{vmatrix} \qquad \Omega = \begin{vmatrix} \theta \\ \Psi \end{vmatrix} \tag{1}$$

is called the Radar Cross Section (RCS) of the target for the frequency f and the illumination angle Ω

2. CLASSICAL RADAR IMAGING

The most popular model developed in radar imaging is the model of white and isotropic bright points [1]. The target is modelized by a set of white and isotropic bright points which respond in a same way for all the frequencies and for all the illumination angles. Let $a(\vec{x})$ be the amplitude of bright point $\vec{x}$, the vector which defines its position in the target coordinates system. The complex backscattering coefficient for the set of bright points becomes:

$$H(\vec{k}) = \int a(\vec{x})\, e^{-2i\pi \vec{k}.\vec{x}}\, d\vec{x} \tag{2}$$

Performing the Fourier transform of H, we obtain the density of the repartition of bright points for a mean frequency (center frequency of the emited bandwidth) and for a mean angle (center angle of the angular analysis extent). The classical and fast techniques of radar imaging are based on the Fourier transform. In this case, only small angular extent around the target is possible in order that $\sin\theta \cong \theta$ and $\cos\theta = 1$ in the relation (2). The new radar imaging technique allows to avoid this problem while keeping a fast and discrete computation algorithm. Moreover, the bright points of the target does not respond in the same way for all the frequencies (colored points) and all the illumination angles (non isotropic points). By removing the classical assumptions, the density $a(\vec{x})$ of the repartition of bright points must depend on the wave vector $\vec{k}$. This operation makes the inversion of the integral transform impossible by classical Fourier transformation techniques:

The group theory, dimensional analysis and wavelet analysis allow to define a radar image for each frequency and angle of illumination [2].

3. RADAR IMAGING BY DIMENSIONALIZED WAVELET TRANSFORM

The group to consider in radar imaging is the similarity group in space (rotations $\Re$, dilations a, translations $\delta\vec{x}$). This group transforms the bright points model in the following way:

$$\begin{aligned} \vec{x} &\longrightarrow \vec{x}' = a\,\Re\,\vec{x} + \delta\vec{x} \\ \vec{k} &\longrightarrow \vec{k}' = a^{-1}\,\Re\,\vec{k} \end{aligned} \tag{3}$$

The complex backscattering coefficient of the target can be considered as the ratio between the reflected field E_r, which can be assimilated to a spherical wave and the incident field E_i which will be always assimilated to a plane wave. This coefficient can be written as [3]:

$$H(f) = \lim_{R\to\infty} \sqrt{4\pi R^2}\; E_r/E_i\; e^{4i\pi fR/c} \tag{4}$$

The square modulus of the coefficient H has the dimension of an area. In a clock change (dilation or contraction of the time), any physical quantity must be corrected in order that any observer who puts up with this clock change has the same measure of this quantity. In our particular case, the SER of the different bright points must be at the same level if the model is reduced by any scale factor and the frequencies increased in the inverse ratio. Thus, in a transformation of the affine group, the complex backscattering coefficient H must be corrected by some power of the compression factor in order to keep coherence between all the observers. The transformation of H by the similarity group leads to:

$$H(\vec{k}) \longrightarrow H'(\vec{k}) = a\; e^{-2i\pi\vec{k}.\delta\vec{x}}\; H(a\;\Re^{-1}\vec{k}) \tag{5}$$

The scale change of length does not change only the coordinates of bright points but also the unit used for the evaluation of H.

The spatial repartition I_m of bright points in the space $\mathbb{R}^m$ (which depends on their spatial localization and on their wave vector), can be viewed as a density, such that its integral $\sigma_V(\vec{k})$ over a space volume V represents the partial contribution of SER of the elements of V. If the dimension of the problem is noted by m (m=1,2,3), then I_m must have the dimension L^{2-m} (L stands for a length), in order that $\sigma_V(\vec{k})$ has an area dimension which characterizes the square modulus of H (SER dimension). Acting with the similarity group, these images must be transformed according to the scheme:

$$I_m(\vec{x},\vec{k}) \longrightarrow I'_m(\vec{x},\vec{k}) = a^{2-m}\; I_m(a^{-1}\Re^{-1}(\vec{x}-\delta\vec{x}), a\Re^{-1}\vec{k}) \tag{6}$$

The factor a^{2-m} is always a dimensional factor which ensures the coherence of the measure of the images. Among all the images I_m, the distributions $L_{\vec{x}_0,\vec{y}_0}$ localized in $(\vec{x}_0,\vec{k}_0)$ which remain localized after

similarity transformation are of the form:

$$L_{\vec{x}_0,\vec{k}_0}(\vec{x},\vec{k}) = A\ k^{m-2}\ \delta(\vec{x}-\vec{x}_0)\ \delta(\vec{k}-\vec{k}_0) \qquad (7)$$

let $\Phi(k,\Omega)$ be a backscattering function of a reference target. Let this function be localized around the origin $\vec{x}=0$, reflect essentially in the direction of the unit vector $\vec{n}$ which defines the unit wave vector $\vec{k}$ for the frequency f=1 and be invariant by all the rotations around $\vec{n}$ axis. By the similarity group and following the transformation scheme given by (3) with $a=1/k_0$, $\delta x=x_0$, $\Re$= rotation of angle Ω_0, a family $\Psi_{\vec{x}_0,\vec{k}_0}(\vec{k})$, called wavelet basis can be generated from the mother wavelet $\phi(k,\Omega)$ in the following way:

$$\Psi_{\vec{x}_0,\vec{k}_0}(\vec{k}) = \frac{1}{k_0}\ e^{-2i\pi\vec{k}.\vec{x}_0}\ \phi(\frac{k}{k_0},\Omega,\Omega_0) \qquad (8)$$

This construction process makes the wavelet basis identical for all the observers and depends only on the mother wavelet of the reference target. We have hence obtained a set of coherent states for the similarity group which can be used for wavelet analysis [5]. The wavelet coefficient $C(\vec{x}_0,\vec{k}_0)$ is therefore introduced as the invariant scalar product between the complex backscattering coefficient H and each element of the wavelet basis:

$$C_m(\vec{x}_0,\vec{k}_0) = (H\ ,\ \Psi_{\vec{x}_0,\vec{k}_0})_m = \int_S d\Omega \int_0^{+\infty} k\ H(k,\Omega)\ \Psi^*_{\vec{x}_0,\vec{k}_0}(\vec{k})\ dk \qquad (9)$$

with $\int_S d\Omega = 1$ in dimension one, $d\Omega = d\theta$ in dimension two and $d\Omega = \cos\Psi\ d\Psi\ d\theta$ in dimension m=3. This invariant scalar product plays an important part because the wavelet coefficient becomes without dimension. This coefficient is therefore the same for all the observers. The main approach of the construction of the images is to interpret, thanks to isometry relation, the square modulus of the wavelet coefficient over its admissibility coefficient as a probability density without dimension in the whole space (x,k). These images can be therefore viewed as a mean of localized states $L_{\vec{x}_0,\vec{k}_0}(\vec{x},\vec{k})$ with the density $p(\vec{x}_0,\vec{k}_0) = |C(\vec{x}_0,\vec{k}_0)|^2 / K_m(\phi)$. This approach gives:

$$I_m(\vec{x},\vec{k}) = |C(\vec{x},\vec{k})|^2\ k^{m-2} / K_m(\phi) \qquad (10)$$

We obtain, for each analysis frequency and each illumination angle, the repartition map of bright points of the target under analysis. We can study the behaviour of the localization of these bright points when frequency and illumination angle change. Finally, for a given frequency and angle, $I_m(\vec{x},\vec{k})\ \Delta\vec{x}$ represents the SER level of the $\vec{x}$ element in a vinicity $\Delta\vec{x}$ of $\vec{x}$.

4. BIDIMENSIONAL RADAR IMAGING

In two dimensions, the complex backscattering coefficient is collected for each frequency and each illumination angle. The repartition map of bright points represents the evolution of their SER level when frequency and illumination angle vary. The chosen wavelet $\phi(f,\theta)$ has the form:

$$\phi(f,\theta) = f^{2\pi\lambda-1}\ e^{-2\pi\lambda f}\ e^{-\theta^2/2\sigma_\theta^2} \qquad (11)$$

where λ is a real parameter of the Klauder wavelet which controls its spread in frequency and σ_θ is the standard deviation which controls its spread in angle. Using the powerful tool of the Mellin transform, all operations to compute numerically (10) for m=2 only need the Fast Fourier Transform algorithm. For a number $N_f N_\theta$ of computed radar images, the whole complexity of this algorithm can be given by $2N_x N_y + 1$ FFT of N_f points and $2N_x N_y + 1$ FFT of N_θ points, if we note N_x the number of points in the radial space, N_y the number of points in the transversal space, N_f the number of points of H collected in frequency space and N_θ the number of points of H in angular space

We now present simulations made in anechoic room on a small target. This one has a length of 60cm and a width of 40cm (Fig. 3) and is illuminated by plane waves. The analysis bandwidth is 8.2-12.4Ghz between -30 and 30 degrees. The complex backscattering coefficient is collected for each geometrical frequency on the analysis bandwidth and for each angle of target presentation. Figures 1 and 2 represent the results obtained with the technique described before for different values of parameters λ and σ_θ. For each series of parameters λ and σ_θ, we have chosen to display only three images among all the $N_f \times N_\theta$ computed. For each image, one can distinguish the nose, the wings, the air intake and the bottom of the missile which are reflecting most of the energy.

The first images series (analysis on [8.2, 12.4] Ghz and [-20°, 20°]) of Fig.1 is obtained for a large frequency width of the wavelet (λ=10) and a large angular width of the wavelet (σ_θ=20°). The three images (a), (b) and (c) are given for the set of parameters (f_0=9Ghz, θ_0=0°), (f_0=10.3Ghz, θ_0=0°) and (f_0=11.3, θ=0°) . It can be noted that the three images are not fundamentally different in frequency (the wavelet has a wide bandwidth) with nevertheless a better range resolution at high frequency. The second images series of Fig.1 represents the same analysis but with narrow-band wavelet (λ=100, σ_θ=30°) on [8.2, 12.4] Ghz and [-10, 10] degrees. Hence, the range resolution is not as good as in the previous series but the bright points localization changes with frequency. These two examples show the duality between good range resolution and good resolution frequency. The third images series of Fig.2 shows the behaviour of the radar images for different angle of target presentation. With a wide angular and frequency extent (λ=10, σ_θ= 20°) wavelet on [8.2, 12.4] Ghz and [-30, 30] degrees, the three images (a), (b) and (c) are obtained for the same frequency f_0=10.3Ghz but for different angles of analysis θ_0=-25°, θ_0=0° and θ_0=25°. It can be noted that the right wing has disappeared for θ_0=-25° and the left one has disappeared for θ_0=25°. The last images series of the figure 2 obtained for λ=10 and σ_θ=5° with analysis on [8.2, 12.4] Ghz and [-20, 20] degrees shows the duality between good angular resolution and good cross-range resolution. The three images (a), (b) and (c) are given for the same frequency f_0=10.3 and different angles of analysis -15°, 0° and 15°

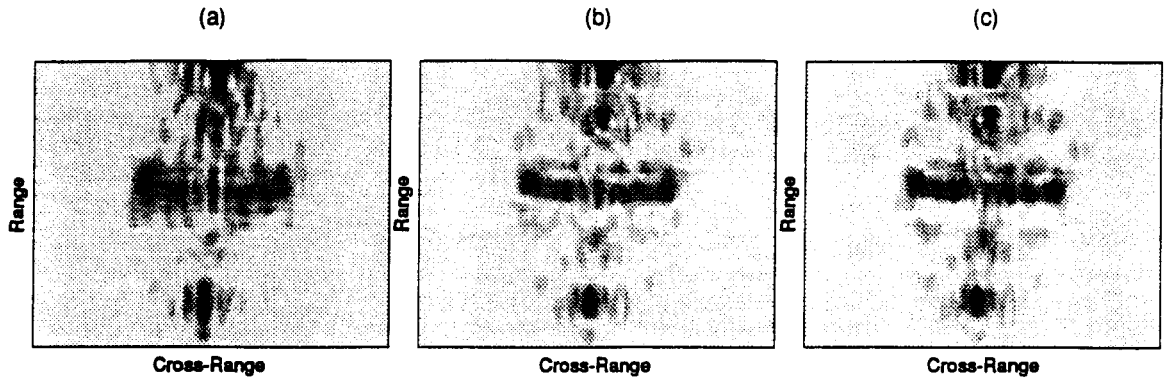

(1) Analysis with a good range and cross range resolutions for a direction of illumination given by $\theta=0$ (poor frequency resolution)

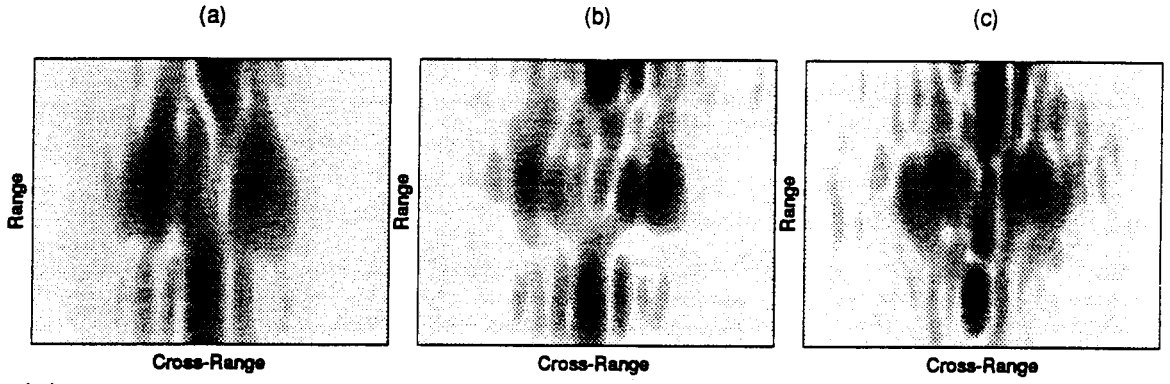

(2) Analysis with a poor range and cross range resolutions for a direction of illumination given by $\theta=0$ (good frequency resolution).

Figure 1: Two dimensional radar images of a missile

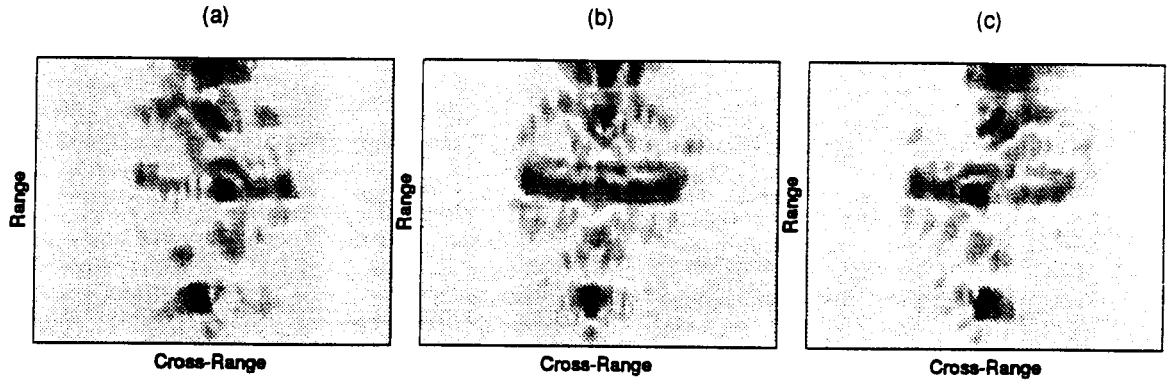

(1) Analysis in frequency and angular domain with a good range and cross range resolutions

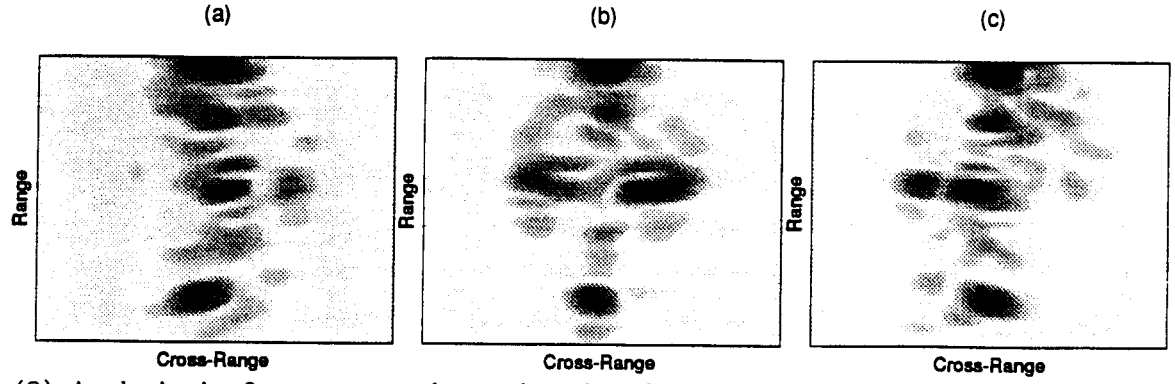

(2) Analysis in frequency and angular domain with a poor range but good cross range resolutions

Figure 2: Two dimensional radar images of a missile

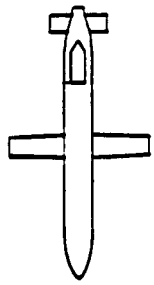

Figure 3: Reduced model of the analysed missile

5. CONCLUSION

This radar imaging technique is interesting for several raisons. The model of bright points is improved. First, the bright points are viewed as colored and non isotropic and their space localization changes with frequency and illumination angle. The dimensional constraints play an important role in wavelet analysis. The measure of the different physical quantities in use must be perfectly coherent for all the observers. Secondly, all the acquisitions of the complex backscattering coefficient are made using a polar discretization. This one is based on a geometric frequency sampling of H and an arithmetic angle sampling. All the transformations used for the images computations need only the Discrete Mellin Transform and only the Discrete Fourier Transform (which need both only a FFT algorithm) and avoid the classical procedure of interpolation between polar space coordinates and cartesian space coordinates. Finally, the Mellin transform has been used successfully in problem concerning wide band signal analysis: fast computation of wide-band ambiguity function, wavelet transform, affine time frequency representation, wide-band radar imaging and theorical computation of the Cramer-Rao bounds in the broad-band case of the velocity estimate [8].

ACKNOWLEDGEMENTS: The authors would like to thank J.C.Castelli for its help in the practical applications and the Service Technique des Programmes Aeronautiques for its financial support

REFERENCES

[1] **D.L.Mensa,** *"High Resolution Radar Cross-Section Imaging"*, Artech House 91
[2] **J.Bertrand, P.Bertrand et J.P.Ovarlez,** *"Dimensionalized Wavelet Transform with Application to Radar Imaging"*, IEEE-ICASSP, Toronto, Canada, May 1991
[3] **J.Bertrand P.Bertrand,** *"Some Practical Aspects of the Affine Time Frequency Distributions"*, XIIIème Col. GRETSI, pp.25-28, Juans les Pins, Sept. 1991
[4] **P.Bertrand, F.Tardivel,** *"Représentation Temps-Fréquence des Signaux et Transformations Affines sur le Temps. Application à un Problème d'Imagerie Radar"*, Xème Col. GRETSI, pp.7-12, Nice, 1985
[5] **R.Murenzi,** *"Wavelet Transforms Associated to the n-Dimensional Euclidian Group with Dilations"*, in *"Wavelets, Time-Frequency Methods and Phase Space"*, J.M.Combes, A.Grossmann and Ph.Tchamitchian (eds), Springer-Verlag (1989)
[6] **J.Bertrand P.Bertrand J.P.Ovarlez,** *"Discrete Mellin Transform for Signal Analysis"*, IEEE-ICASSP 90, pp.1603-1606, Albuquerque (NM), 1990
[7] **J.Bertrand P.Bertrand,** *"Affine Time-Frequency Distributions"*, in *"Time Frequency Signal Analysis - Methods and Applications"*, Ed. B.Boashash, Longman-Cheshire, 1991
[8] **J.P.Ovarlez,** *"La Transformation de Mellin: un Outil pour l'Analyse des Signaux à Large Bande"*, Thèse de Doctorat Université Paris 6, Avril 1992